Available online at www.sciencedirect.com
ScienceDirect
Journal of Power Sources 166 (2007) 485–491
JOURNAL OF POWER SOURCES
www.elsevier.com/locate/jpowsour

Oxygen deficiency, a key factor in controlling the cycle performance of Mn-spinel cathode for lithium-ion batteries

Yonggao Xia, Hongyu Wang, Qing Zhang, Hiroyoshi Nakamura, Hideyuki Noguchi *, Masaki Yoshio

Department of Applied Chemistry, Saga University, 1 Honjo, Saga 840-8502, Japan

Received 1 September 2006; received in revised form 12 January 2007; accepted 13 January 2007
Available online 20 January 2007

Abstract

Several series of $Li_{1\pm x}Mn_{2-y}O_{4\pm\delta}$ and $Li_{1.05}Al_yMn_{1.95-y}O_{4\pm\delta}$ samples with different oxygen defect degree have been synthesized by controlling synthesis temperature and procedures. The cycle performance of spinel as cathode in lithium batteries has been correlated with oxygen deficiency. The structure change of spinel during charge has also been investigated with respect with oxygen deficiency.

Keywords: Al-doped spinels; Cycling performance; Oxygen deficiency; Mn dissolution; Lithium-ion batteries

1. Introduction

Spinel type lithium manganese oxides are the most promising cathode materials for lithium ion batteries because they are cheaper, less toxic and more easily prepared than other candidates (lithium nickel oxides and lithium iron orthophosphate). A problem hindering the practical application of Mn spinel is the capacity fading upon cycling in both spinel/Li and spinel/carbon cells, especially at elevated temperature. Several reasons have been suggested to explain its degraded cycling performance, including structural instability [1–3], Jahn–Teller distortion [4] and Mn dissolution into electrolyte [5–7], etc. But no general consensus for the capacity fading mechanism has yet been reached.

Other than the above reasons, Deng et al. [8,9] recently proposed that oxygen deficiency plays most important role in cycleability. Greatly improved cycling performance could be obtained for Li-rich spinel with oxygen stoichiometry even at elevated temperature. It was also found that oxygen defect degree is reduced as result of Mn dissolution during storage at elevated temperature. Takahashi et al. [10] believed that stabilized structure by reducing the oxygen deficiency contributes to the improvement of 60 °C storage performance of the cell.

In fact, to suppress Mn dissolution from spinel surface in the electrolyte, the surface area of spinel can be made small by the means of sintering at rather high temperatures (over 850 °C). It is likely that oxygen deficiency often presents in extra-heated spinel samples [11,12]. In the charge/discharge profiles for this type of samples, a "fingerprint" 3.2 V discharge plateau usually appears. Gao and Dahn have ascribed the 3.2 V discharge plateau to oxygen deficiency and suggested to use it as a "qualitative indicator for detecting oxygen deficiency" [12].

We have verified the quantitative relationship between the capacity of 3.2 V discharge plateau and oxygen defect degree. To further the insights on the influence of oxygen deficiency, we attempt to correlate the oxygen defect degree to capacity fading in detail. In this study, we have prepared series of Mn-spinel and Al doped Mn-spinel with different oxygen defect degree by strictly controlling the synthesis conditions. The effects of oxygen deficiency on the structure change as well as the cycle performance have bee addressed.

2. Experimental

The undoped spinel samples were prepared by melt-impregnation method as follows. The mixture of Mn_3O_4 (Tosoh, Japan) and LiOH was pre-calcined 500 °C for 5 h in air, and then post-calcined at the temperature range of 700–900 °C in air.

* Corresponding author. Tel.: +81 952 28 8674; fax: +81 952 28 8591.
E-mail address: noguchih@cc.saga-u.ac.jp (H. Noguchi).

0378-7753/$ – see front matter © 2007 Published by Elsevier B.V.
doi:10.1016/j.jpowsour.2007.01.023

Two series of $Li_{1+x}Al_yMn_{2-x-y}O_{4\pm\delta}$ ($x = 0.05$, $y = 0.05, 0.10$ and 0.15) samples were prepared by two different methods, respectively. The N series samples were prepared by a two-step solid state reaction: (1) in the first step; the mixture of LiOH, Mn_3O_4 and Al_2O_3 (in mole ratio of 1:1.95:0.05, 1:0.9:0.10 and 1:0.85:0.15 for N-Al005-660, N-Al010-660 and N-Al015-660, respectively) was sintered at 500 °C for 5 h and then calcinated at above 1000 °C for 10 h to get the intermediate product with small surface area; (2) in the second step; the extra LiOH (0.05 for 1.0 LiOH in the staring material) was added into the intermediate product and then annealed at 660 °C to get the final product. Another C series samples designed as C-Al005-*T*, C-Al010-*T* and C-Al015-*T* ("*T*" is 800, 850, 900, 950 or 1000 corresponding to the calcination temperature) with almost the same Al content of N-Al005-660, N-Al010-660 and N-Al015-660 were prepared by the conventional one-step method [2].

The chemical composition of as-prepared samples was determined by chemical analysis, and some results were listed in Table 1. The details of chemical analysis were described in the previous paper [13].

The structures of the samples were characterized by XRD (Rigaku Rint 1000) using Cu Kα radiation.

The electrochemical performance of spinel was evaluated using CR2032 coin-type cells. Cathodes were prepared by mixing Mn-spinels with 8 wt% polyvinylidene fluoride (PVDF) and 4 wt% acetylene black (AB). The slurry mixture was coated on an Al foil and then pressed. Unless specified otherwise, lithium metal was used as an anode and glass fiber (GA-100) as the separator (Toyo Roshi Kaish, Ltd., Japan). The electrolyte was 1 M $LiPF_6$-ethylene carbonate/dimethyl carbonate (EC/DMC, 1:2 by volume) (Ube Industries, Ltd., Japan). Cells were galvanostatically charged and discharged with a cut-off voltage range of 3–4.3 V versus Li/Li^+ at room temperature (RT) and 60 °C.

To investigate the reaction mechanism that occurs in the spinels material, *ex situ* XRD patterns were collected on the spinel electrodes at selected capacity points during the initial charge. The cells were dismantled in an Ar-filled glove box, and then the spinel electrodes were recovered and washed by DMC solvent to remove the salt. After the evaporation of DMC, the electrodes were covered by a thin transparent waterproof paraffin film and were subjected to XRD measurement. XRD data of spinel electrodes were collected in the range of $2\theta = 10$–$80°$ with a step of 0.02°.

Table 1
Summary for the Al-doped spinels in the present paper

Sample name	Chemical composition	Average Mn valance	Prepared method
C-Al005-1000	$Li_{1.033}Al_{0.049}Mn_{1.918}O_{3.990}$	3.545	One-step method
C-Al010-1000	$Li_{1.035}Al_{0.110}Mn_{1.855}O_{3.994}$	3.570	One-step method
C-Al015-1000	$Li_{1.041}Al_{0.148}Mn_{1.811}O_{3.997}$	3.594	One-step method
N-Al005-660	$Li_{1.035}Al_{0.053}Mn_{1.912}O_{3.993}$	3.552	Two-step method
N-Al010-660	$Li_{1.038}Al_{0.097}Mn_{1.865}O_{3.999}$	3.576	Two-step method
N-Al015-660	$Li_{1.039}Al_{0.146}Mn_{1.815}O_{4.017}$	3.613	Two-step method

3. Results and discussion

3.1. The effect of oxygen defect degree on the electrochemical performance and structure of Li–Mn–O spinels

We consider that the oxygen-defect spinel has Schottoky type oxygen defect as shown in Fig. 1. Above structure is supported by crystallographic studies [14], one oxygen vacancy give rise to three Mn ions with the coordination number of 5 (MnO_5), which links with three MnO_6 octahedrons across O atom. Therefore, 1 mol defect oxygen forms 12 Mn atoms (three sets of MnO_5–$(MnO_6)_3$), which contribute to the two equivalent plateaus at 3.2 and 4.5 V. Here, these capacities are expressed as $C_{3.2\,V}$ and $C_{4.5\,V}$, respectively. Assume that the molar ratio of $Mn^{3+}/(Mn^{3+} + Mn^{4+})$ is 0.5 and 1 mol Mn^{3+} in $LiMn_2O_4$ delivers 148 mAh g^{-1} capacity, we could obtain the following equation for the capacity of 12δ mole Mn in $LiMn_2O_{4-\delta}$: $C_{3.2\,V} + C_{4.5\,V} = 148 \times 12\delta \times 0.5$. Since $C_{3.2\,V}$ equals to $C_{4.5\,V}$, $C_{3.2\,V}$ could be expressed as

$$C_{3.2\,V} = 148 \times 12\delta \times 0.5 \times 0.5 = 444\delta \quad (1)$$

In order to further confirm the accuracy of the above equation, based on the data of previous paper [15] and the present work, we plot the $C_{3.2\,V}$ against 444δ as shown in Fig. 2. The linear relationship in this figure would strongly support our suggestion, which is based on the crystallographic reason.

The relation between cycling performance and oxygen defect degree for Li–Mn–O spinel system can be seen in Fig. 3, where

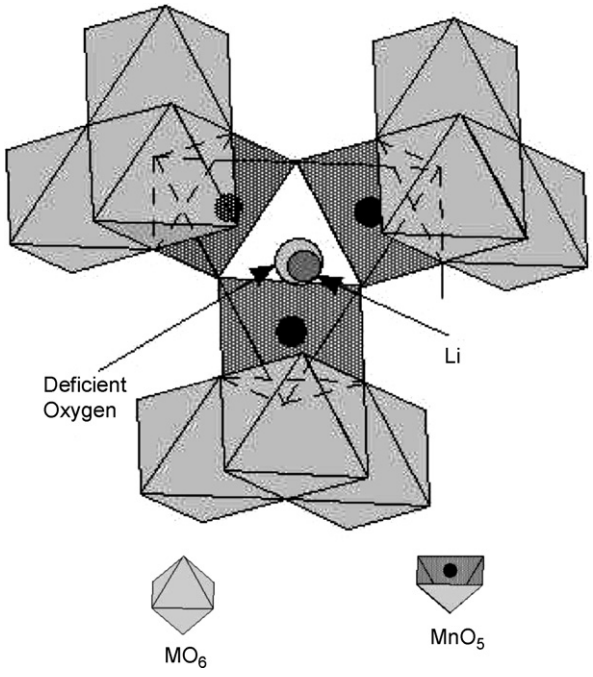

Fig. 1. Structure of oxygen deficient spinel.

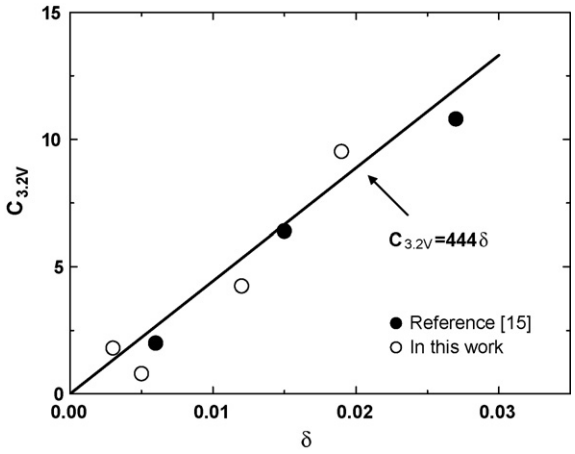

Fig. 2. Relationship between $C_{3.2}$ and δ.

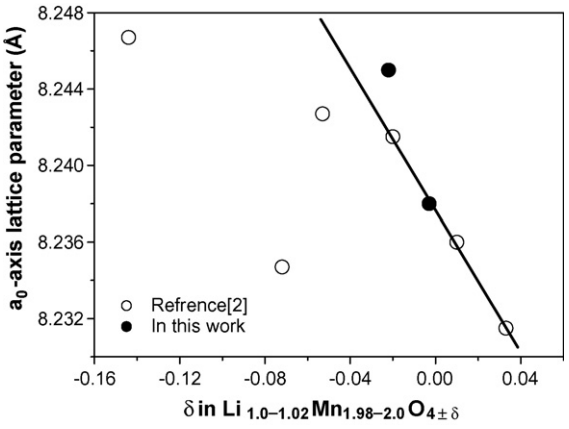

Fig. 4. The effect of δ on lattice parameter of in $Li_{1.0–1.02}Mn_{1.98–2.0}O_{4\pm\delta}$.

the capacity retention after the first 50 cycles along with various oxygen defect degree δ were described. Besides the four painted circles applied in our previous paper [13], four open circles were added in the present work. All the points are distributed around a straight line. It shows an almost relationship between oxygen defect degree and the capacity fading, and the capacity retention C_{50}/C_1 could be express as follows: $C_{50}/C_1 = (100 - 2.17 \times 10^3\delta)/100$. Moreover, the extrapolation of this line to $\delta = 0$ could give the crossover point of 100%. Therefore, it would indicate that the most important factor for improving cycleability is oxygen stoichiometry in spinel cathode material when the spinel cathode was cycled at room temperature.

The lattice parameters are also influenced by oxygen deficiency. Fig. 4 shows the relation between lattice parameter and δ in spinel compounds. It is clear that lattice parameters of Li–Mn–O spinel increase with the increase in oxygen content. The intersect point at $\delta = 0$ is 8.237 Å would be the accurate lattice parameter of the ideal $LiMn_2O_4$.

The different electrochemical performance, including capacity and recharge-ability might be due to the difference in electrometrical Li^+-intercalation mechanisms. To investigate the changes in the crystal structure during charge, XRD examinations were performed on both oxygen stoichiometric spinel and oxygen defect spinel. The cubic lattice parameter for oxygen stoichiometric spinel, lithium rich spinel with oxygen stoichiometry and oxygen defect spinel as a function of lithium content, z, in $Li_{1-z}Mn_2O_4$ are plotted in Fig. 5(A)–(C), respectively. It is evident in Fig. 5(C) that, in the range of $0 < z < 0.2$, the a_0 retains the constant value of 8.25 Å, which could be considered as the two-phase coexist region. Moreover, two crystal phases with different lattice parameters still present in the range of $0.5 < z < 1$. These results show clear evidence of two-phase coexistence regions on both the 4.0 and 4.2 V plateau, in agreement with the three cubic model proposed by Yang et al. [16].

Fig. 5(A) shows that the a_0-axis shrinks almost linearly from 8.247 to 8.125 Å in the region for $0 < z < 0.5$. This is very differ-

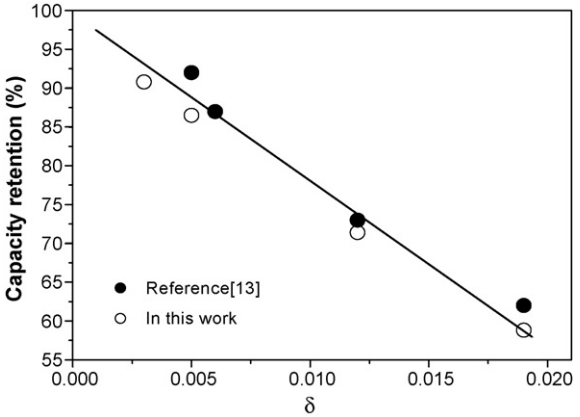

Fig. 3. Dependence of capacity retention after first 50 cycles and oxygen deficiency degree (δ) for undoped spinel. Current density: 0.4 mA cm^{-2}; voltage rang: 3.0–4.3 V; room temperature.

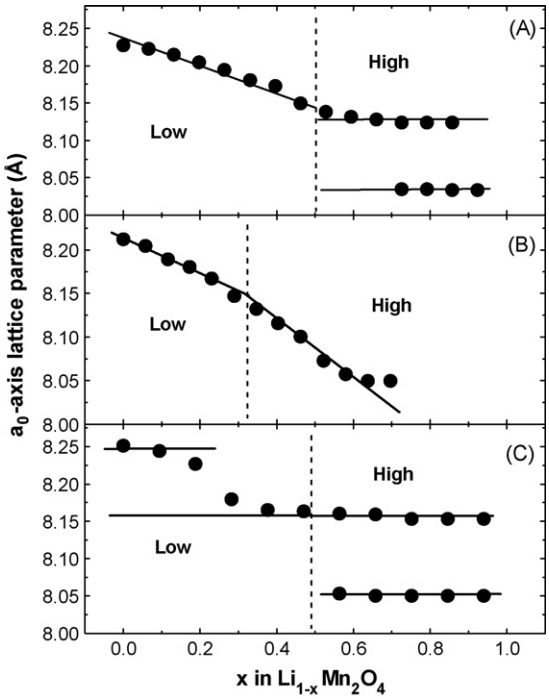

Fig. 5. Variation of the a_0-axis lattice parameter at different charge states for oxygen stoichiometric spinel (A), lithium rich spinel with oxygen stoichiometry (B), and oxygen deficient spinel (C), respectively.

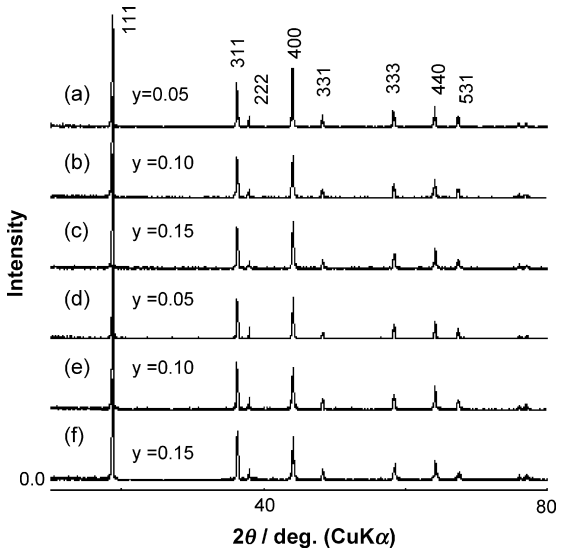

Fig. 6. XRD patterns for the $Li_{1.05}Al_yMn_{1.95-y}O_4$ ($y = 0.05$, 0.10 and 0.15) materials prepared by the conventional one-step method (a–c) and two-step method (d–f).

ent from the oxygen defect sample, where two-phase coexistence in the same region. The different unit-cell lattice change patterns during charge and discharge in this region mainly results in the different electrochemical properties between oxygen stoichiometric spinel and oxygen defect spinel. It further confirmed that the capacity fading during cycling for oxygen defect spinel occurs on both 4.0 and 4.2 V plateau. In contract, this fading occurs on 4.2 V plateau only for the spinel without an oxygen deficiency. These results are in good agreement with the result reported by Xia and Yoshio [2].

On the other hand, Fig. 5(B) shows that a_0 decreases almost linearly from 8.22 to 8.15 Å in the region of $0 < z < 0.3$, and then decreases almost linearly from 8.15 to 8.05 Å in the region of $0.3 < z < 0.8$. This can be considered as the one-phase model proposed by Xia and Yoshio for lithium-rich samples [2]. It should be noted that there are no two-phase coexistence in $z > 0.55$, which is very different from the Fig. 5(A) and (C). We suggest that excess lithium could suppress the phase transitions at all region. In altering the lithium and oxygen content by different annealed temperature and synthesis procedures, we have successfully reproduced the results for the one-, two-, and three-phase models. This clearly demonstrates that the structural changes during charge/discharge cycling are determined by the Li/Mn ratio and the oxygen deficiency. Between these two factors, the oxygen deficiency is the primary cause and the ratio of Li/Mn is secondary.

3.2. The effect of oxygen defect degree on the electrochemical performance and structure for Al doped Mn-spinel

Fig. 6 shows the XRD patterns of spinel samples $Li_{1.05}Al_yMn_{1.95-y}O_{4\pm\delta}$ ($y = 0.05$, 0.10 and 0.15) prepared by conventional method and two-step method. All the diffraction peaks can be indexed on the cubic structure with the space group $Fd\bar{3}m$ and there are no peaks of impurity phase.

Fig. 7 shows the initial two charge/discharge curves of Li/$Li_{1.05}Al_yMn_{1.95-y}O_{4\pm\delta}$ cells using the two series of samples as cathode materials. A plateau at 3.2 V correlated with oxygen deficiency was observed for C-Al005-1000 ($Li_{1.033}Al_{0.049}Mn_{1.918}O_{3.990}$), C-Al010-1000 ($Li_{1.035}Al_{0.110}Mn_{1.855}O_{3.994}$), C-Al015-1000 ($Li_{1.041}Al_{0.148}Mn_{1.811}O_{3.997}$)

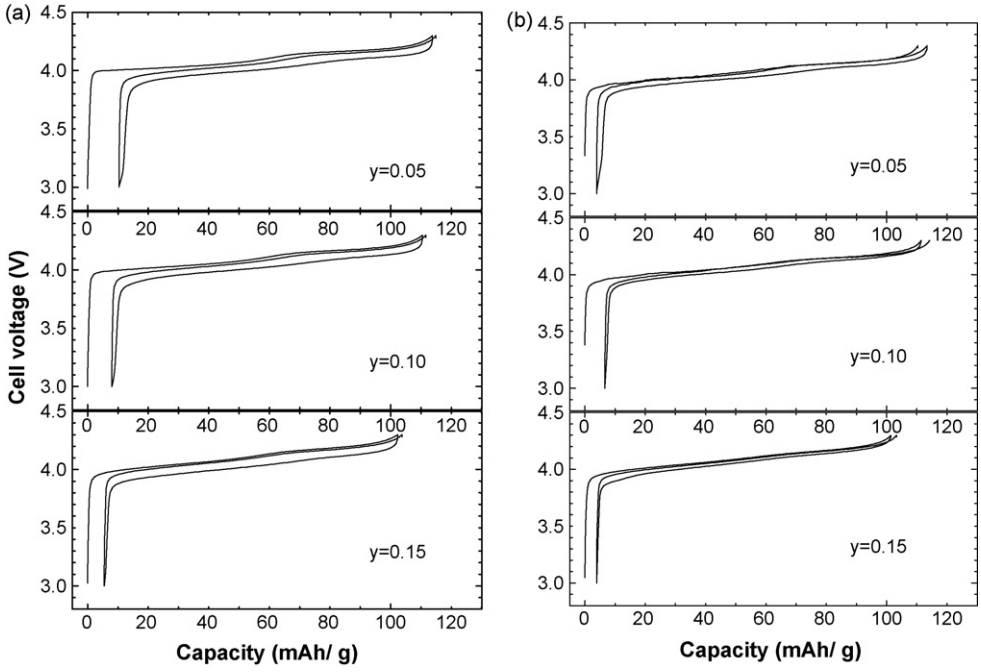

Fig. 7. Charge/discharge curves at room temperature of $Li_{1.05}Al_yMn_{1.95-y}O_4$ ($y = 0.05$, 0.10 and 0.15) by different method: (a) conventional method and (b) two-step method. The current density: 0.1 mA cm^{-2}.

and N-Al005-660 ($Li_{1.035}Al_{0.053}Mn_{1.912}O_{3.993}$). This means that the oxygen deficiency still exist even at the doping amount of Al as high as 0.15 in the case of the conventional one-step method. However, for two-step method, oxygen defect spinel was found only at the low doping level of $y = 0.05$. When the doped Al content is 0.15, the chemical formula of N-Al015-660 determined by $Li_{1.039}Al_{0.146}Mn_{1.815}O_{4.017}$, and it could be called as oxygen stoichiometric spinels with cation vacancies in 16d site and rewritten as $[Li]_{8a}[Li_{0.035}Al_{0.145}Mn_{1.807}\square_{0.013}]_{16d}[O_4]_{32e}$ ($\square$ denotes cation vacancies). This formula indicates that sintering with extra LiOH at 660 °C can repair the oxygen deficiency originating from sintering at high temperature. It is also noted that the polarization of samples prepared by two-step is smaller than those of samples prepared by the conventional one-step method.

The cycling performance of N-Al015-660, N-Al010-660 cathodes were tested and shown in Fig. 8. For comparison, the two controlled materials C-Al015-1000 and C-Al010-1000, with almost the same Al doping content as N-Al015-660 or N-Al010-660, are shown in the same figure. The capacities of C-series samples fade more rapidly than those of N-series samples with no oxygen deficiency. Oxygen stoichiometric sample N-Al015-660 exhibits excellent cycleability, and loses only 0.66% of the capacity even after the 50 cycles, whereas the C-Al015-1000 sample with a slight oxygen deficiency loses 8% of initial capacity, although they have almost the same Al content and specific surface area. C-Al010-1000 with the largest oxygen deficiency among the four samples exhibits the poorest cycling performance; it loses ca. 15% of initial capacity after 50 cycles. On the other hand, N-Al010-660 exhibits better cycling behavior although the Al doping content of C-Al015-1000 is higher than that of N-Al010-660. It is probably due to difference in oxygen content of both samples, because the chemical analysis shows that $4 \pm \delta$ value in (Li, Al and Mn)$_3O_{4\pm\delta}$ (oxygen contents) is 3.999 for N-Al010-660 and 3.997 for C-Al015-1000, respectively.

The relation between cycling performance and the degree of oxygen defect can be more clearly observed in Fig. 9, where the capacity retention after 50 cycles at 60 °C is plotted against

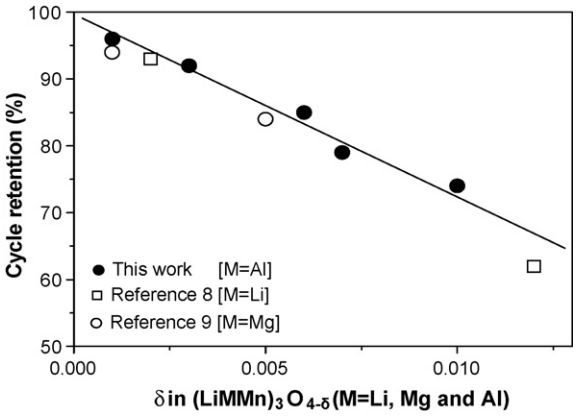

Fig. 9. Dependence of capacity retention after first 50 cycles and oxygen deficiency degree (δ). Current density: 0.4 mA cm^{-2}; voltage range: 3.0–4.3 V; 60 °C.

the oxygen defect degree δ. Beside four painted circles obtained form the present work, four open marks were added in our previous study [8,9]. Although the kind of doping metal is different, the capacity retentions give a linear line against the oxygen defect degree δ. The capacity retention C_{50}/C_1 at 60 °C could be reduced as follows: $C_{50}/C_1 = (100 - 2.75 \times 10^3\delta)/100$. It shows that the capacity fading of high temperature is more significant than that of room temperature ($100 - 2.16 \times 10^3\delta$). When δ is extrapolated to 0, the capacity retention would achieve ca. 100%, which is very similar to Fig. 3. Consequently, we confirm that the oxygen stoichiometry is a determining factor in cycleability improvement in spite of ambient temperature. In fact, Al-doping can help the increase in the oxygen content in the spinel when they was synthesized in the same condition, and it turns to improve the cycling performance of spinel samples.

Fig. 10 shows the *ex situ* XRD patterns for N-Al015-660 ($Li_{1.039}Al_{0.146}Mn_{1.815}O_{4.017}$) cathode during the initial charge from 3.0–4.3 V under galvanostatic condition of 0.4 mA cm^{-2}. All the diffraction peaks move to higher angles in a continuous fashion during charge. Further, it is confirmed that the *ex situ* XRD patterns of Al doped oxygen defect spinel C-Al005-

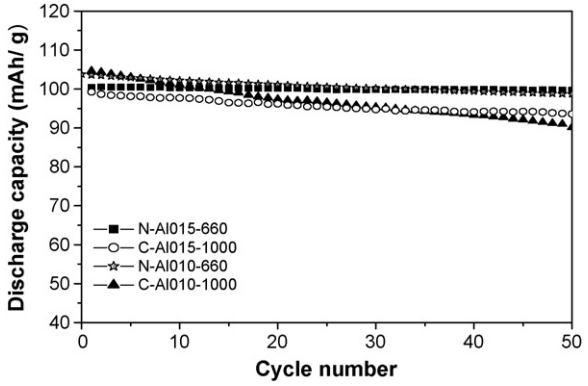

Fig. 8. The cycling performance of N-Al015, C-Al010-1000, C-Al015-1000 and N-Al010 cathodes at 60 °C (0.4 mA m^{-2}).

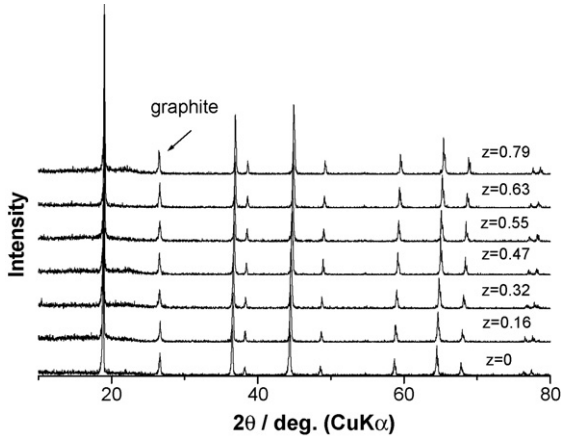

Fig. 10. The *ex situ* XRD patterns for N-Al015-660 cathode at different charge states.

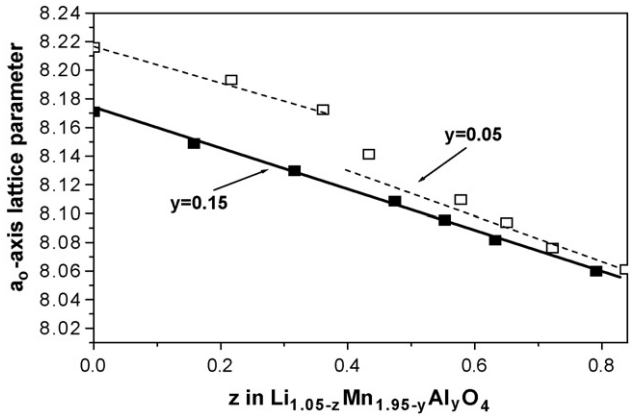

Fig. 11. Variation of the *a*-axis lattice parameter for N-Al015-660 and C-Al005-1000 cathode at different charge states.

1000 ($Li_{1.033}Al_{0.049}Mn_{1.918}O_{3.990}$) also are similar to those of N-Al-660 during charge process. This behavior is quit different from that of normal Li–Mn–O spinel with oxygen deficiency [2], which gives two-phase mechanism in both low and high voltage regions of charge process. In other words, electrochemical processes of Al doped oxygen defect spinels are completely different from those of normal oxygen defect Li–Mn–O spinel. Moreover, there are no any new peaks during cycling, so it is suggested that the crystal structure is very stable in the charge process.

In order to obtain more detailed information for the structure of two typical spinels, cubic lattice parameters of both samples were calculated and plotted as a function of z in Fig. 11. The unit cell sizes of de-lithiated oxygen stoichiometric spinel, $Li_{1.039-z}Al_{0.146}Mn_{1.815}O_{4.017}$, shrink uniformly from 8.17 to 8.06 Å and the shape of the curve is expressed as one continuous line. Similar results have been also reported in the $LiMn_{1.95}M_{0.05}O_4$ (M = B and Ni) compounds [17]. On the other hand, the curve of oxygen defect spinel, $Li_{1.033-z}Al_{0.049}Mn_{1.918}O_{3.990}$, is composed of two continuous lines divided at ca. $z = 0.4$. Both lines are roughly parallel with that of oxygen stoichiometric spinel. The cell sizes of oxygen defect spinel in the region of $z < 0.4$ are 0.04 Å larger than those of oxygen stoichiometric spinel, however, both spinels give roughly same sizes in the region of $z > 0.5$. Sudden shrinkage attacks oxygen defect spinel at around $z = 0.4$. We believe this impact causes the instability of crystal during the cycling. Moreover, the doped spinel with oxygen defect exhibits larger volume change ($\Delta a_0/\Delta z = 0.18$) in all region than that of Lee's [17], who reported that the volume change in $LiMn_{1.95}Al_{0.05}O_4$ is 0.13–0.14 when the sample prepared at relatively low temperature of 800 °C. Such large volume change is essentially due to larger cell size of oxygen defect spinels because the delithiate products have the same unit cell volume. In fact, volume change of our oxygen stoichiometric spinel is also about 0.13 in all regions. Moreover, a comparison of Figs. 11 and 3 reveals that the phase transition evolving at $x > 0.55$ in undoped spinel is greatly suppressed by Al doping. In the previous paper [1,2], we have suggested that the structure of spinel collapses due to the lattice stress imposed by the phase transition occurring in all regions for oxygen defect undoped spinel. Therefore, the excellent cycling performance of this sample may also be correlated with the absence of a phase transition.

4. Conclusions

In this study, *ex situ* XRD has further indicated the cause of capacity fading in various kinds of spinels. It shows clearly that two-phase coexistence region occurs on both the 4.0 and 4.2 V plateau for undoped spinel with oxygen deficiency. This behavior is quite different from the undoped spinel with oxygen stoichiometry, where two-phase coexistence region occurred on the 4.2 V plateau region only. However, Al doped spinel with oxygen stoichiometry shrink uniformly from 8.17 to 8.06 Å during de-lithiation, which could be considered as one-phase reaction. Furthermore, we have confirmed that the capacity retentions give a linear line against the oxygen defect degree δ in normal spinel at room temperature, as well as Al doped spinel at 60 °C. When δ is extrapolated to 0, the capacity retention would achieve ca. 100% in both cases.

We have successfully prepared oxygen-stoichiometric spinel by sintering a mixture of Mn_3O_4, LiOH and Al_2O_3 at 1000 °C and then annealing at lower temperature together with extra LiOH. This new sample exhibits excellent capacity retention. The capacity retention of the new kind of oxygen-stoichiometric spinel is about 99.34% at 60 °C in the half-cell after 50 cycles. To the best of our knowledge, this is the best value among the reported papers. It is believed that the new kind of Al doped spinel is a promising cathode materials for practical applications.

Acknowledgement

This work was financially supported by the New Energy and Industrial Technology Development Organization (NEDO), Japan.

References

[1] Y. Xia, M. Yoshio, J. Electrochem. Soc. 143 (1996) 825.
[2] Y. Xia, T. Sakai, T. Fujieda, X. Yang, X. Sun, Z. Ma, J. McBreen, M. Yoshio, J. Electrochem. Soc. 148 (2001) A723.
[3] S.J. Wen, T.J. Richardson, L. Ma, K.A. Striebel, P.N. Ross, E.J. Cairns, J. Electrochem. Soc. 143 (1996) L136.
[4] R.J. Gummow, A. de Kock, M. Thackeray, Solid State Ionics 69 (1994) 59.
[5] D.H. Jang, Y.J. Shin, S.M. Oh, J. Electrochem. Soc. 143 (1996) 2204.
[6] Y. Xia, M. Yoshio, J. Electrochem. Soc. 144 (1997) 4186.
[7] A. Blyre, C. Sigala, G. Amatucci, D. Guyomard, Y. Chabre, J.M. Tarascon, J. Electrochem. Soc. 145 (1998) 194.
[8] B. Deng, H. Nakamura, M. Yoshio, Electrochem. Solid-State Lett. 8 (2005) A171.
[9] B. Deng, H. Nakamura, Q. Zhang, M. Yoshio, Y. Xia, Electrochim. Acta 49 (2004) 1823.
[10] M. Takahashi, T. Yoshida, A. Ichikawa, K. Kitoh, H. Katsukawa, Q. Zhang, M. Yoshio, Electrochim. Acta 51 (2006) 5508.
[11] J.M. Tarascon, W.R. McKinnon, F. Coowar, T.N. Bowmer, G. Amatucci, D. Guyomard, J. Electrochem. Soc. 141 (1994) 1421.
[12] Y. Gao, J.R. Dahn, J. Electrochem. Soc. 143 (1996) 100.
[13] X. Wang, H. Nakamura, M. Yoshio, J. Power Sources 110 (2002) 19.

[14] R. Kanno, A. Kondo, M. Yonemura, R. Gover, Y. Kawamoto, M. Tabuchi, T. Kamiyama, F. Izumi, C. Masquelier, G. Rousse, J. Power Sources 81/82 (1999) 542.
[15] Y. Yagi, Y. Hideshima, M. Sugita, H. Noguchi, M. Yoshio, Electrochemistry 68 (2000) 252.
[16] X.Q. Yang, X. Sun, S.J. Lee, J. McBreen, S. Mukerjee, M.L. Daroux, X.K. Xing, Electrochem. Solid-State Lett. 2 (1999) 157.
[17] J.H. Lee, J.K. Hong, D.H. Jang, Y.-K. Sun, S.M. Oh, J. Power Sources 89 (2000) 7.